Catalysis Today 146 (2009) 166–171

Contents lists available at ScienceDirect

Catalysis Today

journal homepage: www.elsevier.com/locate/cattod

Combined H_2O and CO_2 reforming of CH_4 over nano-sized Ni/MgO-Al_2O_3 catalysts for synthesis gas production for gas to liquid (GTL): Effect of Mg/Al mixed ratio on coke formation

Kee Young Koo [a], Hyun-Seog Roh [b,*], Un Ho Jung [a], Dong Joo Seo [a], Yong-Seog Seo [a], Wang Lai Yoon [a,**]

[a] *Strategic Technologies Research Division, Korea Institute of Energy Research (KIER), 71-2, Jang-dong, Yuseong, Daejeon 305-343, Republic of Korea*
[b] *Department of Environmental Engineering, Yonsei University, 234, Maeji, Heungeop, Wonju, Gangwon-do 220-710, Republic of Korea*

ARTICLE INFO

Article history:
Available online 12 March 2009

Keywords:
Gas to liquid (GTL)
Combined reforming
Ni/MgO-Al_2O_3
Coke resistance
SMSI

ABSTRACT

Nano-sized Ni catalysts were prepared by using MgO-Al_2O_3 mixed oxides from hydrotalcite-like structure as a support. The property of support was controlled with various Mg/Al mixed ratio to enhance coke resistance in combined H_2O and CO_2 reforming of CH_4 (CSCRM) to produce synthesis gas (H_2/CO = 2) for gas to liquid (GTL). 12% Ni/MgO-Al_2O_3 catalyst with Mg/Al of 0.5 shows the highest activity in CSCRM due to high coke resistance, resulting from nano-sized Ni particles strongly interacting with the support.

1. Introduction

The synthesis gas production for gas to liquid (GTL) process attracts an increasing interest in combined steam and carbon dioxide reforming of methane (CSCRM) which is a feasible process to adjust the H_2/CO ratios of syngas with various feed ratio of H_2O and CO_2 [1–4]. In general, the required H_2/CO ratio of syngas depends on the target processes such as Fischer–Tropsch (F–T) and methanol synthesis [5]. When the conventional steam reforming and dry reforming processes are applied for the syngas production for GTL, these processes need an additional process to adjust the H_2/CO ratio [6–9]. In addition, the commercial auto-thermal reforming and partial oxidation of methane to produce the syngas (H_2/CO = 2) for F–T synthesis have some drawbacks such as follows. These reforming processes require the oxygen plant which is very expensive and have difficulty in process control due to explosion danger [10,11]. Therefore, the effective syngas production is required to overcome the drawbacks of conventional reforming processes. In this study, the syngas production for the F–T synthesis was carried out in CSCRM by controlling the feed H_2O/CO_2 ratio.

In these reforming processes, Ni-based catalysts have been used as promising catalysts because of high activity comparable to expensive noble metal catalysts. In general, Ni catalysts deactivate rapidly due to carbon deposition and metal sintering in severe operating conditions [12,13]. It is inevitable to develop the highly dispersed nano-sized Ni catalysts with strong metal to support interaction (SMSI) which results in high coke resistance and prevents the metal sintering [14]. In addition, it has been reported that the addition of a basic metal oxide into the catalyst improved coke resistance [15]. In this study, Ni catalysts supported on hydrotalcite-like MgO-Al_2O_3 have been used as promising catalysts. These mixed oxides prepared by hydrotalcite compounds have been investigated because of some advantages such as thermal stability, large surface area and well dispersion of metal catalyst (Ni) [16,17]. Tsyganok et al. [18] reported that the preparation methods of Ni containing Mg–Al layered double hydroxides (LDH) have an effect on the coke deposition and the state of the supported nickel. Hou and Yashima [19] reported that mesoporous Ni/Mg/Al catalysts prepared by coprecipitation method exhibited high activity and low coke formation because the highly dispersed Ni catalysts with SMSI prevent the coke formation and sintering. We have also reported that the surface area and NiO crystallite size depend on the pre-calcination temperature of support in nano-sized Ni/MgO-Al_2O_3 catalysts obtained from hydrotalcite-like material in CSCRM [2].

Base on the results of our previous work, the effect of Mg/Al ratio on coke resistance has been investigated in CSCRM since the surface properties such as basicity of support and structure depends on the Mg/Al ratio. In addition, the optimum Mg/Al ratio for coke resistance has been discussed in coke study using SEM, TGA analysis and Raman spectroscopy.

---

* Corresponding author.
** Corresponding author. Fax: +82 33 763 5224/42 860 3739.
E-mail addresses: hsroh@yonsei.ac.kr (H.-S. Roh), wlyoon@kier.re.kr (W.L. Yoon).

0920-5861/$ – see front matter © 2009 Elsevier B.V. All rights reserved.
doi:10.1016/j.cattod.2009.02.002

2. Experimental

2.1. Catalyst preparation

$Ni/MgO\text{-}Al_2O_3$ catalysts were prepared by the incipient wetness method using the hydrotalcite-like $MgO\text{-}Al_2O_3$ mixed oxide (Mg/Al molar ratio = 0.5, 1.3, 3.5, SASOL) and nickel nitrate (97%, JUNSEI). Supports were pre-calcined in air at 800 °C for 6 h. The loading amount of Ni was fixed at 12 wt%. The catalysts were calcined in air at 800 °C for 6 h.

2.2. Characterization

The crystal structure and compositional homogeneity of the prepared catalysts were examined by X-ray diffraction (XRD, Rigaku D/Max-III C, Cu Kα radiation). The surface area of each catalyst was measured by BET (Micromeritics, ASAP 2000) through the nitrogen adsorption at −196 °C. H_2-chemisorption was performed by using pulse technique to identify the metallic dispersion and metal surface area in BEL-METAL-3 (BEL Japan, Inc.). The sample of 50 mg was reduced in H_2 flow at 700 °C for 1 h. The sample was purged at 700 °C for 1 h in He flow and cooled to 50 °C. A hydrogen pulse (20% H_2/Ar) was injected into the catalyst. The adsorbed H_2 amount obtained by assuming the adsorption stoichiometry of one hydrogen atom per nickel surface atom ($H/Ni_{surface} = 1$) was used to estimate Ni dispersion and surface area.

Temperature programmed reduction (TPR, Micromeritics, Autochem 2910) was carried out to identify the reduction temperature and H_2 consumption of catalysts. The sample of 0.1 g in a quartz reactor was pre-treated with He gas at 250 °C for 1 h, then cooled down to 50 °C, and then re-heated by an electrical furnace at heating rate of 20 °C/min from 100 to 1000 °C under 10% H_2 in Ar gas. The sensitivity of the detector was calibrated by reducing known weight of NiO. The reduction degree was estimated by integrating the peak area of the reduction profile relative to the reference curve of NiO [2]. To estimate the reduction degree in the same reduction condition prior to the reforming reaction, the peak area of the TPR profile was integrated up to 700 °C.

CO_2-temperature programmed desorption (CO_2-TPD, Bel-Metal) was performed to identify the basic strength distribution of the support. The sample of 50 mg in a quartz reactor was pre-treated with He gas at 700 °C for 1 h and then cooled down. CO_2 was adsorbed at 50 °C for 1 h and weakly adsorbed CO_2 was removed by purging with He. The sample was heated from 50 to 900 °C at a heating rate of 10 °C/min in He flow and the desorbed amount of CO_2 was detected with a thermal conductivity detector (TCD). The CO_2 amount was estimated by integrating the TPD profile with the Distribution Fitting Software (BEL Japan, Inc.).

2.3. Catalytic test

The CSCRM was carried out from 750 to 650 °C over 15 h under atmospheric pressure. Before the reaction, the catalyst was reduced at 700 °C for 1 h with 10% H_2 in N_2. To obtain the syngas with H_2/CO ratio of 2, the reforming reaction was performed with the feed ratio of $CH_4:H_2O:CO_2:N_2 = 1:0.8:0.4:1$ at GHSV = 530,000 ml/(h g_{cat}) from 750 to 650 °C. In our previous work, we have reported that the H_2/CO ratio was controlled by the feed ratio of H_2O and CO_2 [20]. To clarify the catalytic activity according to the Mg/Al molar ratio, we compared the initial CH_4 conversion with the final CH_4 conversion of each catalyst after reforming test under severe condition (GHSV = 1,060,000 ml/(h g_{cat})) at 700 °C for 15 h. The effluent was passed through a trap to condense residual water and then analyzed with an on-line micro gas chromatograph (Agilent 3000) equipped with a TCD detector. In this study, CSCRM to obtain the syngas with $H_2/CO = 2$ involves the following reaction:

$$3CH_4 + 2H_2O + CO_2 \rightarrow 8H_2 + 4CO$$

H_2 and CO yields are defined as follows:

$$H_2\ \text{yield}\ (\%) = \frac{\text{Experimental}\ H_2\ \text{product}}{\text{Theoretical}\ H_2\ \text{product}} \times 100$$

$$\text{CO yield}\ (\%) = \frac{\text{Experimental CO product}}{\text{Theoretical CO product}} \times 100$$

2.4. Coke study

The coke test was carried out under severe conditions resulting in the deactivation of the catalyst to observe the coke formation on the catalyst related with the effect of Mg/Al ratio. The prepared catalysts with various Mg/Al molar ratios were loaded in a fixed-bed reactor without diluents. After reforming test under condition of GHSV = 530,000 ml/(h g_{cat}) at 650 °C for 15 h, the used catalysts were collected. The detailed reaction procedure was described in our previous report [3]. The morphologies and coke formation of used catalyst were identified by scanning electron microscopy (SEM, Philips XL30SREG). The quantitative analysis of coke amount on the used catalyst was performed with a thermogravimetry analyzer (TGA, Netzsch TG209F3). The sample of 50–70 mg was heated from 30 to 800 °C with a heating rate of 5 °C/min in air. The Raman spectra were obtained with a LabRam HR spectrometer (Horiba Jobin Yvon) using a 514 nm excitation source. A 100 μm pinhole was used with the spectral resolution grating, yielding about 1.0 cm^{-1} resolution.

3. Results and discussion

3.1. Catalyst characterization

Fig. 1(a) shows the XRD patterns of pre-calcined $MgO\text{-}Al_2O_3$ supports with various Mg/Al molar ratios. $MgO\text{-}Al_2O_3$ mixed oxide which consists of the Mg/Al molar ratio of 0.5 was transformed into $MgAl_2O_4$ spinel phase after pre-calcination at 800 °C. At the Mg/Al molar ratio of 1.3, the MgO phase co-exists with $MgAl_2O_4$, while MgO peaks are dominant with Mg/Al of 3.5. It is obvious that the MgO phase becomes dominant by increasing the Mg/Al molar ratio. From the XRD patterns of $Ni/MgO\text{-}Al_2O_3$ catalysts, it is hard to distinguish the MgO peak from the NiO peak because the peaks overlap each other in Fig. 1(b).

Fig. 2 shows the H_2-TPR patterns of $Ni/MgO\text{-}Al_2O_3$ catalyst with various Mg/Al molar ratios. The peak appearing at 800 °C is assigned to the reduction peak of complex NiO_x species, which have strong interaction with support [2]. In the case of catalyst with Mg/Al = 0.5, TPR peak is present at high temperature (830 °C) due to SMSI. As the Mg/Al molar ratio increases, TPR peaks are present at high temperature above 900 °C resulting from formation of NiO-MgO solid solution [21,22]. As a result, the $Ni/MgO\text{-}Al_2O_3$ catalysts with higher Mg/Al molar ratio can be partially reduced under reduction condition at 700 °C for 1 h due to the fact that the catalysts can be completely reduced above 900 °C. It is clear that the reduction degree of prepared catalysts is different (Table 1).

Table 1 summarizes the characteristics of the $Ni/MgO\text{-}Al_2O_3$ catalysts with various Mg/Al molar ratios. In this table, H_2 uptake of $Ni/MgO\text{-}Al_2O_3$ catalyst with Mg/Al molar ratio of 0.5 is the highest, resulting in the highest Ni surface area (3.4 m^2/g). With increasing the Mg/Al ratio, reduction degree of Ni decreases. This is due to the fact that solid solution formation of NiO-MgO obstructs the reduction of NiO species, resulting in less available Ni sites after

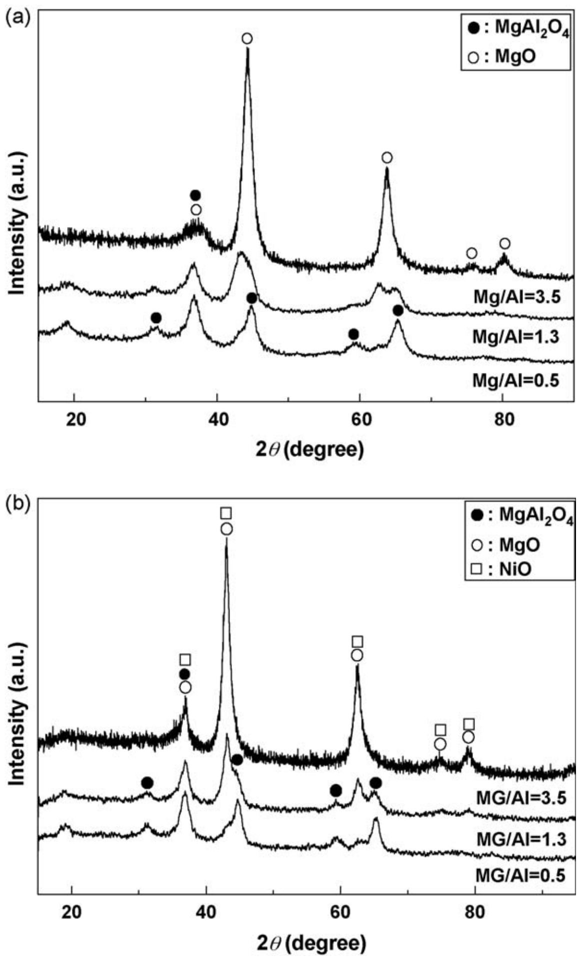

Fig. 1. XRD patterns of pre-calcined MgO-Al_2O_3 supports (a) and Ni/MgO-Al_2O_3 catalysts and (b) with various Mg/Al molar ratios.

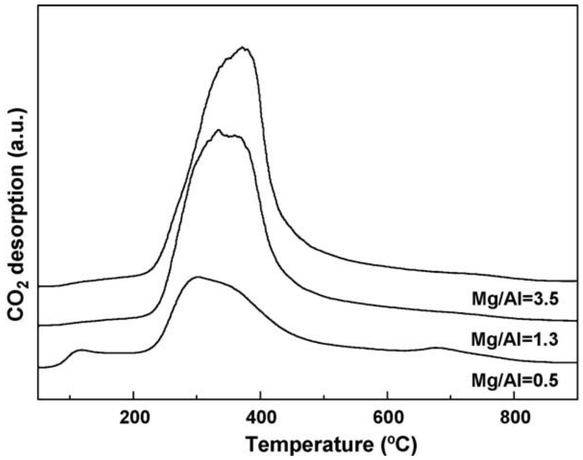

Fig. 3. CO_2-TPD patterns of Ni/MgO-Al_2O_3 catalysts with various Mg/Al molar ratios.

the reduction process. As expected from the TPR results, Ni catalyst is partially reduced due to formation of a NiO-MgO solid solution.

Fig. 3 shows the CO_2-TPD patterns of Ni/MgO-Al_2O_3 catalysts with various Mg/Al molar ratios. In the case of the catalyst with Mg/Al ratio of 0.5, three types of basic site exist at 115, 305 and 680 °C. On the other hand, TPD peaks of catalysts with Mg/Al ratio of 1.3 and 3.5 show a separate peak at 345 and 365 °C, respectively. As the Mg/Al ratio increases, TPD peaks shift toward the high temperature and show higher peak intensity attributed to the increase of basicity. The total amount of desorbed CO_2 was estimated from the integration of CO_2-TPD peak area (Table 2). In the case of the catalyst prepared with Mg/Al molar ratio of 0.5, the amount of desorbed CO_2 is 1 mmol/g at 115 °C, 9.8 mmol/g at 305 °C and 3 mmol/g at 680 °C, respectively. The CO_2-TPD result demonstrates that the basicity of prepared catalysts increases obviously with the increase of Mg/Al molar ratio. In general, the basic catalysts could improve the adsorption of acidic CO_2 gas which supplies the surface oxygen to suppress the coke deposition [21,23]. In addition, the basicity and strength of basic sites of the catalyst have an effect on the catalytic performance [24]. In this study, the catalyst with Mg/Al molar ratio of 0.5 shows high catalytic activity and good coke resistance as compared to other catalysts with high basicity. This can be explained as follows. Tang et al. [25] reported that prior to weak basic sites, strong basic sites are favorable to depress the coke formation in MgO and CaO promoted Ni catalysts. In our study, the catalyst with Mg/Al = 0.5 has the weak, middle and strong basic sites whereas other catalysts have the only middle basic site. As a consequence, the high coke resistance of the catalyst with Mg/Al = 0.5 is possibly related to the presence of strong basic site at 680 °C. However, it is hard to evaluate the catalytic activity and coke resistance by the difference of basic strength because the catalytic performance depends on the various factors including the Ni metal size, dispersion, reduction degree and so on.

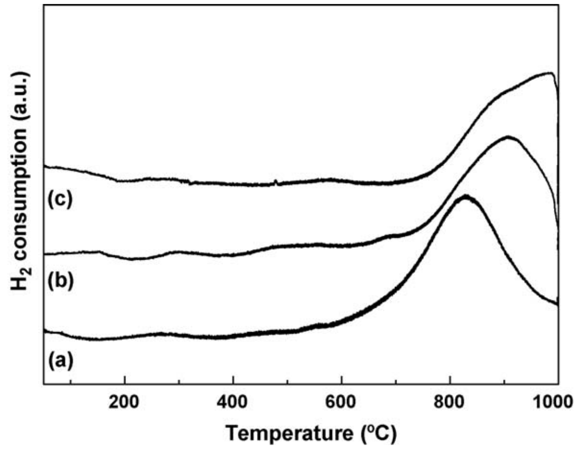

Fig. 2. H_2-TPR patterns of Ni/MgO-Al_2O_3 catalysts with various Mg/Al molar ratios of 0.5 (a), 1.3 (b) and 3.5 (c).

Table 1
Characteristics of Ni/MgO-Al_2O_3 catalysts with various Mg/Al molar ratios.

Mg/Al molar ratio	BET S.A.[a] (m^2/g)	H_2 uptake[b] (μmol/g_{cat})	Reduction degree[c] (%)	Ni dispersion[b] (%)	Ni surface area[b] (m^2/g)	Ni size[b] (nm)
0.5	108	42.1	14.6	27.5	3.4	3.5
1.3	112	32.2	9.6	31.5	2.6	3.1
3.5	100	23.2	2.5	90.8	1.9	1.1

[a] Estimated from N_2 adsorption at −196 °C.
[b] Estimated from H_2-chemisorption at 50 °C.
[c] Calculated from reduction of the catalysts at 700 °C for 1 h.

Table 2
CO_2-TPD results of Ni/MgO-Al_2O_3 catalysts with various Mg/Al molar ratios.

Mg/Al	0.5	1.3	3.5
Total desorbed CO_2 [a] (mmol/g)	13.8	20.8	24.0

[a] Estimated from the integration of CO_2-TPD peaks.

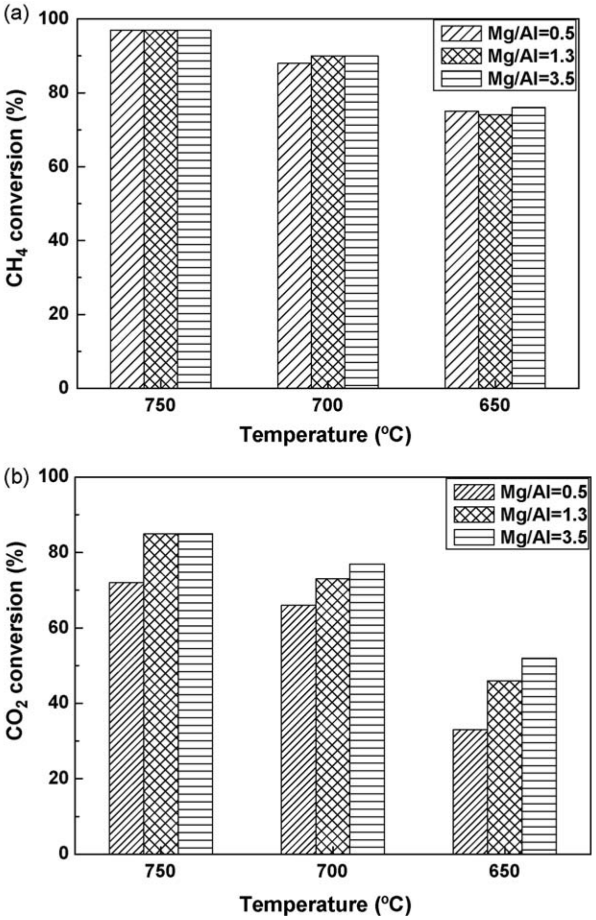

Fig. 4. CH_4 conversion (a) and CO_2 conversion (b) with reaction temperature over Ni/MgO-Al_2O_3 catalysts with various Mg/Al molar ratio (reaction conditions: CH_4:H_2O:CO_2:N_2 = 1:0.8:0.4:1, GHSV = 530,000 ml/(h g_{cat})).

3.2. Catalytic test in CSCRM

Fig. 4 shows the results for CH_4 conversion and CO_2 conversion with different reaction temperature from 750 to 650 °C. All the catalysts exhibited almost thermodynamic equilibrium CH_4 conversion within a range of acceptable error, while the CO_2 conversion showed some difference at 650 °C. The Mg/Al molar ratio of 3.5 showed the highest CO_2 conversion. It is most likely that the increase of Mg/Al molar ratio is favorable to CO_2 adsorption, resulting in the increase of CO_2 conversion. Table 3 summarizes the H_2 and CO yield and H_2/CO ratio over Ni/MgO-Al_2O_3 catalysts with various Mg/Al molar ratios at 750 °C in CSCRM. These values are almost close to the thermodynamic equilibrium values. It is noted that CO yields of catalysts with Mg/Al molar ratio of 1.3 and 3.5 are above 100% because of the reverse water gas shift reaction (RWGS: $CO_2 + H_2 = CO + H_2O$) at high temperatures. The selectivities to both H_2 and CO are 100% because there is no side product in CSCRM [21]. It has been confirmed that the H_2/CO ratio of 2.0 which is required for the F–T synthesis is achieved by CSCRM.

Table 3
Reaction results over Ni/MgO-Al_2O_3 catalysts at 750 °C in CSCRM.

Mg/Al ratio	H_2 yield (%)	CO yield (%)	H_2/CO
0.5	96.2	97.3	2.0
1.3	94.8	101.6	2.0
3.5	94.6	102.2	2.0

All the reactions were carried out at GHSV = 530,000 ml/(h g_{cat}).

Table 4
CH_4 conversion over Ni/MgO-Al_2O_3 catalyst with Mg/Al molar ratio of 0.5 and 3.5.

	Mg/Al = 0.5	Mg/Al = 3.5
Initial CH_4 conversion (%)	85	78
Final CH_4 conversion (%)	65	60

All the reactions were carried out at GHSV = 1,060,000 ml/(h g_{cat}).

To screen the catalysts more rapidly, the GHSV was doubled to 1,060,000 ml/(h g_{cat}) at 700 °C. At this condition, we compared initial CH_4 conversion with final conversion (time on stream = 15 h). Table 4 summarizes the initial conversion and final conversion. The CH_4 conversion dropped with time on stream. Ni/MgO-Al_2O_3 catalyst (Mg/Al = 0.5) exhibited higher CH_4 conversion than that with a ratio of 3.5. As pointed out previously, the highly dispersed Ni particle with SMSI offers resistance to sintering and coke deposition. The lower CH_4 conversion of catalysts with Mg/Al ratio of 3.5 is attributed to low Ni surface area due to low

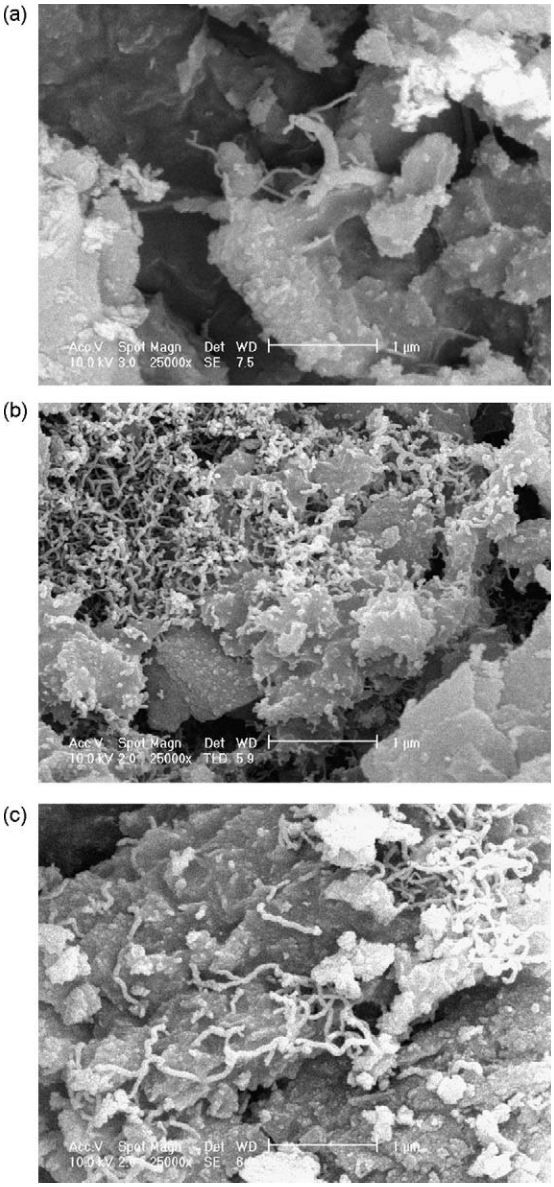

Fig. 5. SEM images of used catalysts with Mg/Al molar ratio of 0.5 (a), 1.3 (b) and 3.5 (c).

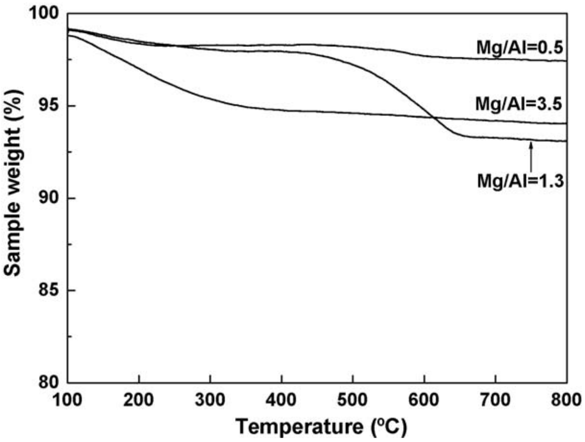

Fig. 6. TG profiles of used Ni/MgO-Al_2O_3 catalysts under air.

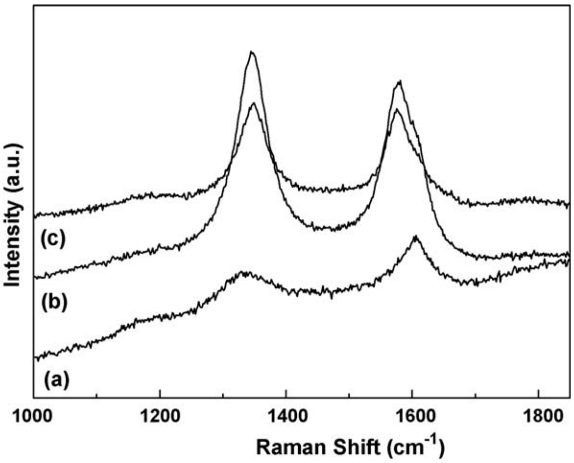

Fig. 7. Raman spectra of the cokes over used Ni/MgO-Al_2O_3 catalysts with Mg/Al molar ratio of 0.5 (a), 1.3 (b) and 3.5 (c).

reducibility of Ni particles, resulting from formation of NiO-MgO solid solution.

3.3. Coke study

The coke formation over used catalysts was monitored by SEM analysis (Fig. 5). It is clear that Ni/MgO-Al_2O_3 catalyst (Mg/Al = 0.5) shows less coke formation, while a lot of filamentous carbon species are present on Ni/MgO-Al_2O_3 catalyst (Mg/Al = 1.3). TGA analysis was carried out to confirm quantitatively the coke amount of used catalysts (Fig. 6 and Table 5). There are drastic loss in sample weight in the catalyst with Mg/Al of 1.3 and 3.5. Moreover, the TGA profiles show the different behavior of weight loss. Tsyganok et al. [18] demonstrates the different behavior of TGA profiles according to the temperature. Below 350 °C, the initial weight loss is ascribed to thermal desorption of H_2O and CO_2 adsorbed and removal of easily oxidizable amorphous coke. Above 500 °C, the weight loss can be assigned to the oxidation of coke to CO and CO_2 (CO_x). It is noted that the increase of weight due to the oxidation of nickel particles on the surface is not observed in used catalysts. It indicates that the Ni particles on the surface of prepared catalysts are hard to oxidize. As pointed out previously, TGA results support that the catalyst with Mg/Al = 0.5 shows high coke resistance resulting from highly dispersed Ni catalyst with SMSI.

The structure and the crystallite size of coke on used catalysts were identified by Raman spectroscopy (Fig. 7). In all used catalysts, two peaks appear in the vicinity of 1350 and 1580 cm^{-1}, respectively. According to some previous reports, the Raman spectrum of graphite in single crystal appears in the 1500–1700 cm^{-1}, which is called G band. On the other hand, the spectrum of polycrystalline and imperfect graphite appears at about 1350 cm^{-1}, which is called the D band [26,27]. The ratio of areas of I_D/I_G is inverse proportion to the crystallite size of the graphite. Based on Jawhari's report [28], the crystallite size of graphite is estimated and summarized in Table 5. The crystallite size of graphite for all catalysts is between 3.36 and 3.65 nm. However, filamentous carbon does not affect the catalytic activity and causes the breakage of catalyst and pressure drop in the reactor [29]. Guo et al. [30] reported that catalytic activity showed no deactivation in spite of a large amount of coke deposition. We also observed that all catalysts maintained high CH_4 conversions irrespective of the coke formation (Fig. 4). At severe condition (GHSV = 1,060,000 ml/(h g_{cat})), the catalyst with Mg/Al = 0.5 showed higher CH_4 conversion than the catalyst with Mg/Al = 3.5 due to the highly dispersed Ni crystallites with SMSI. When the Mg/Al molar ratio increases, it is hard to reduce the Ni catalysts because of formation of NiO-MgO solid solution. These results confirm that Mg/Al = 0.5 is an optimum molar ratio to suppress coke formation. It is most likely that Mg/Al = 0.5 shows optimum SMSI for the highly dispersed Ni crystallites, and forms relatively stable $MgAl_2O_4$ without formation of NiO-MgO solid solution. In addition, it is confirmed that the distribution and strength of basic sites of the catalyst have a significant effect on coke resistance. As a result, catalyst with Mg/Al = 0.5 exhibits the highest activity with stability resulting from high coke resistance.

Table 5
Quantitative data and Raman spectrometry data of carbon deposited on used Ni/MgO-Al_2O_3 catalysts.

Mg/Al ratio	Total amount of coke (%)	I_G/I_D	Crystallite size of graphite[a] (nm)
0.5	1.75	0.765	3.36
1.3	6.14	0.829	3.65
3.5	4.76	0.799	3.52

[a] Estimated from I_G/I_D using crystallite size (nm) = 4.4[I_G/I_D].

4. Conclusion

The nano-sized Ni/MgO-Al_2O_3 catalysts with high coke resistance have been prepared successfully for CSCRM by using mixed oxide with hydrotalcite-like structure as a support. In the case of high Mg/Al molar ratio, formation of NiO-MgO solid solution obstructs the reduction of NiO species, resulting in less available Ni sites after the reduction process. Ni/MgO-Al_2O_3 catalyst with Mg/Al ratio of 0.5 exhibits good catalytic activity and high coke resistance resulting from the stable $MgAl_2O_4$ formation and highly dispersed Ni crystallites with an optimum SMSI.

References

[1] F. Yagi, R. Kanai, S. Wakamatsu, R. Kajiyama, Y. Suehiro, M. Shimura, Catal. Today 104 (2005) 2.
[2] K.Y. Koo, H.-S. Roh, Y.T. Seo, D.J. Seo, W.L. Yoon, S.B. Park, Int. J. Hydrogen Energy 33 (2008) 2036.
[3] K.Y. Koo, H.-S. Roh, Y.T. Seo, D.J. Seo, W.L. Yoon, S.B. Park, Appl. Catal. A 340 (2008) 183.
[4] H.-S. Roh, K.Y. Koo, U.D. Joshi, W.L. Yoon, Catal. Lett. 125 (2008) 283.
[5] X. Song, Z. Guo, Energy Covers. Manage. 47 (2006) 560.
[6] H.-S. Roh, K.W. Jun, W.S. Dong, J.S. Chang, S.E. Park, Y.I. Joe, J. Mol. Catal. A 181 (2002) 137.
[7] P. van Beurden, On the catalytic aspects of steam-methane reforming, a literature survey, ECN (2004) 1–27.
[8] S. Wang, G.Q. Lu, G.J. Millar, Energy Fuels 10 (1996) 896.

[9] H.-S. Roh, H.S. Potdar, K.W. Jun, Catal. Today 93–59 (2004) 39.
[10] A.T. Ashcroft, A.K. Cheetham, M.L.H. Green, P.D.F. Vernon, Nature 35 (1991) 225.
[11] A.C.W. Koh, L. Chen, W.K. Leong, B.F.G. Johnson, T. Khimyak, J. Lin, Int. J. Hydrogen Energy 32 (2007) 725.
[12] J. Sehested, Catal. Today 111 (2006) 103.
[13] D.L. Trim, Catal. Today 49 (1999) 3.
[14] Q.H. Zhang, Y. Li, B.Q. Xu, Catal. Today 98 (2004) 601.
[15] K. Tomishige, Y. Chen, K. Fujimoto, J. Catal. 181 (1999) 91.
[16] O.W. Perez-Lopez, A. Senger, N.R. Marcilio, M.A. Lansarin, Appl. Catal. A 303 (2006) 234.
[17] T. Ohi, T. Miyata, D. Li, T. Shishido, T. Kawabata, T. Sano, K. Takehira, Appl. Catal. A 308 (2006) 194.
[18] A.I. Tsyganok, T. Tsunoda, S. Hamakawa, K. Suzuki, K. Takehira, T. Hayakawa, J. Catal. 213 (2003) 191.
[19] Z. Hou, T. Yashima, Appl. Catal. A 261 (2004) 205.
[20] H.-S. Roh, K.Y. Koo, J.H. Jeong, Y.T. Seo, D.J. Seo, Y.-S. Seo, W.L. Yoon, S.B. Park, Catal. Lett. 117 (2007) 85.
[21] V.R. Choudhary, B.S. Uphade, A.S. Mamman, Appl. Catal. A 168 (1998) 33.
[22] V.R. Choudhary, A.S. Mamman, Appl. Energy 66 (2000) 161.
[23] L. Xiancai, W. Min, L. Zhihua, H. Fei, Appl. Catal. A 290 (2005) 81.
[24] V.R. Choudhary, S.A.R. Mulla, B.S. Uphade, Fuel 78 (1999) 427.
[25] S.-B. Tang, F.-L. Qiu, S.-J. Lu, Catal. Today 24 (1995) 253–255.
[26] A. Shamsi, J.P. Baltrus, J.J. Spivey, Appl. Catal. A 293 (2005) 145.
[27] J. Guo, H. Lou, X. Zheng, Carbon 45 (2007) 1314.
[28] T. Jawhari, A. Roid, J. Casado, Carbon 33 (1995) 1561.
[29] J.R. Rostrup-Nielsen, in: J.R. Anderson, M. Boudart (Eds.), Catalysis Science and Technology, vol. 5, Springer-Verlag, Berlin, 1984 , p. 74 (Chapter 1).
[30] J. Guo, H. Lou, H. Zhao, D. Chai, X. Zheng, Appl. Catal. A 273 (2004) 75.